

## AEROELASTIC DESIGN AND FLIGHT TEST EVALUATION OF THE EXPERIMENTAL AIRCRAFT X-31A

Johannes Schweiger  
Deutsche Aerospace AG  
Military Aircraft Division  
81663 Munich, Germany

Steven K. Dobbs  
Rockwell International  
North American Aircraft Operations  
EL Segundo, Calif., U.S.A.

### Abstract

The X-31A is an experimental demonstrator aircraft developed to explore controlled flight beyond stall. It was designed, manufactured, and tested in a joint effort between U.S. and German agencies and companies.

This paper describes the aeroelastic aspects of the program during all phases, starting with preliminary design considerations, constraints with respect to budget and time schedules, design analysis methods and models, ground tests, and the flight test evaluation.

### Background

The X-31A (Fig. 1) is an experimental demonstrator aircraft developed to explore the maneuverability and flying qualities at high angles of attack and beyond stall limits. Thrust vectoring for pitch and yaw control is accomplished by deflecting three vanes at the aft fuselage into the engine exhaust plume.

In the tradition of famous X-planes <sup>(1)</sup> in over four decades, the X-31A is the first one that was developed and tested within an international cooperation. The funding for the program was split between the United States and German Government, the industrial partners are Rockwell International (RI) in El Segundo and Deutsche Aerospace AG (DASA) in Munich. Full scale design started in 1987, first flight was in 1990 and the flight test program was successfully completed in 1993. An extension of the program is currently being negotiated between both countries. A program overview is given in ref. <sup>(2)</sup>.

### Introduction

Main objectives of the X-31A program were the demonstration of maneuverability in post-stall flight and enhanced agility in the conventional flight regime. It was an additional goal to demonstrate that such an experimental aircraft can be designed and built in a short time for a small amount of money. These constraints as well as the shared design

responsibilities required some new and unconventional approaches to achieve all objectives.

With respect to aeroelasticity, it was a very short time between the start of the full-scale development in 1987 and first flight in 1990 to cover all required design analysis aspects, perform the necessary ground tests and demonstrate aeroelastic integrity for the certification prior to first flight.

### Work Share

While Rockwell International was responsible for the design and manufacturing of the fuselage, canards, and vertical tail structure, DASA designed and built the wings and thrust vectoring vanes.

Structural dynamic and aeroelastic analysis and test activities for the complete airplane were performed by RI with contributions from DASA for the wings and vanes as well as for the flight control system, which was developed under DASA responsibility.

To exchange analysis models and data between both companies, satellite data transmission was used to a vast extent. This approach required detailed specifications for the analysis program codes, data formats, and interfaces between component models and the complete aircraft model.

Because of the 9 hours time difference between California and Germany, direct telecommunication between the two partner companies was limited to a very short time every day. After this handicap was partially resolved by the exchange of information by telefax and computer data through satellite link, the disadvantage could sometimes even be turned into an advantage: the time difference could be

used to save time by working on the same topic in two shifts.

### Approach for the Aeroelastic Design

A detailed description of all aeroelastic design activities is presented in ref. <sup>(3)</sup>.

Because of the limited time and in order to keep the costs low, no flutter wind tunnel model could be built and tested for the verification of analytical models and methods. Instead of this, the airplane was designed for high margins of safety in flutter speed. Instead of the usual 32 percent margin in dynamic pressure, 44 percent were chosen. In a first step, a coarse finite element model of the complete airplane was used during the pre-design phase by RI for the sizing of the structural components by means of mathematical optimization, using the RI program RSOP (Rapid Structural Optimization). Based on these results, a refined NASTRAN finite element model, fig. 2, was created for the detailed design and analysis of the individual components.

Steady and unsteady aerodynamic loads as well as mass distributions for the airplane were based on the RI Unified Panel Method with one common model, depicted in fig. 3. Based on this model and on structural influence coefficients (SIC's) from the NASTRAN structural model, static load cases, including static aeroelastic effects were created for the different design phases, based on flight conditions from the flight simulator. This approach made it possible to include static aero-elastic effects on the aerodynamic pressure distribution simultaneously while the critical load case were identified, rather than correcting rigid aerodynamic loads in an additional analysis loop, as it used to be done in the past.

The major components could then be

designed and analysed independently by applying the correct boundary conditions at the interfaces from the complete model.

For the structural analysis and design optimization of the wing at DASA, the common NASTRAN model was used. Based on the actual design concept, this model was updated to reflect changes like the addition of internal spars or their relocation.

The DASA structural optimization and analysis program LAGRANGE<sup>(4)</sup> was used for the strength and static stability (buckling) design, for static aeroelastic analysis, and for flutter investigation. Fig. 4 shows the final wing model.

### Aeroelastic Design Requirements

#### Flutter Requirements

Although a supersonic capability up to Mach 1.3 was desired as a fall-out, the basic requirements for flutter were Mach 0.9 and a maximum dynamic pressure of 485 kts at sea level (38 kPa).

Because no dedicated transonic flutter investigations were possible, the known transonic dip in flutter speed was predicted with existing data from other airplanes. Fig. 5 shows these values. A reduction factor of 0.79 in dynamic pressure was finally chosen for the X-31A at Mach 0.9.

For the free-play of control surfaces, the requirements from MIL-8870 were applied.

#### Control Surface Buzz Criteria

This single-degree-of-freedom flutter phenomenon usually establishes minimum stiffness requirements for control

surface actuators. Because off-the-shelf equipment should be used as much as possible for the X-31A, it was agreed to investigate the probability of buzz for the control surfaces and the selected actuators, and, in case of a risk, include provisions for buzz dampers in the design.

Fig. 6 summarizes buzz criteria from different agencies and companies and shows the occurrence of buzz from several airplanes.

### Static Aeroelastic Requirements

Because of the direct approach to include static aeroelastic effects in the calculation of pressure distribution and in the simulation of the aircraft's flying qualities and performances, the impacts from static aeroelastic deformations on loads and performances could directly be observed during the structural design. In addition, static aeroelastic effectiveness data was also checked for the clamped component models. Table 1 summarizes wing effectiveness values.

### Structural Dynamic Analysis

As mentioned above, a coarse finite element model for the complete airplane was used during preliminary design studies. The main purpose of this model was the sizing of the structure for static load cases.

For dynamic analysis of the complete airplane and for clamped component analysis for canard and vertical tail, Rockwell used the aerodynamic model as the basic system. The stiffness of the structural models was transformed into this system by means of structural influence coefficients (SICs). The coefficients for these flexibility matrices were generated with NASTRAN by means of multi-point-constraint (MPC) equations.

## Flutter Analysis

### Complete Airplane Analysis at Rockwell

The mass distributions for these models were also generated for the basic aerodynamic system by the weight groups from both companies, using a special Rockwell program system. The approach to derive the mass matrix coefficients is also described in ref. (3) in details.

This approach was also used for the more refined structural models during the complete design phase.

At DASA the same approach was used to provide SICs and mass data from the wing for the complete airplane analysis. In parallel, the dynamic analysis for the wing component at DASA was also performed with the structural model directly, using NASTRAN and LAGRANGE. To generate the proper mass distribution for this model, the masses of the structural components were used directly. Additional masses for the structure, not covered by the elements, were distributed to the grid points by concentrated (lumped) masses, adjusted to match the calculated masses of all structural components. For non-structural masses, different sets of concentrated masses were also added to this model. These sets were based on the actual weights group's data, and were subdivided into groups like electrical or hydraulic installations.

In addition, the 'official' mass data sets were also used for the wing to investigate the origin of differences between the two approaches, between the stiffness and mass data sets being used, or between analysis methods.

After the ground vibration test (GVT), the dynamic model was updated to match test results. This process is also described in details in ref. (3).

With mass and flexibility data derived for the aerodynamic system as described above, and unsteady aerodynamic generalized forces calculated by the doublet lattice method, the flutter analysis were performed with a Rockwell modal, "k"-method program. This program contains root tracking and automatic match point-location subroutines and it automatically interpolates generalized aerodynamic forces for reduced frequencies  $k$  between input values. This process is repeated until the calculated flutter speed is consistent with the selected Match number. The "match point" corresponds with an altitude for the proper air density.

### Wing Component Analysis at DASA

Different models and methods were used at DASA for the clamped wing flutter analysis. Based on the structural grid from the FEM and an aerodynamic doublet lattice model similar to the basic RI model, the NASTRAN p-k-method was used at DASA. In addition, the new LAGRANGE flutter method, developed by Hr. Gödel (4) was tested. For a set of aerodynamic influence coefficient matrices (AICs) at different Mach numbers and reduced frequencies, this method automatically interpolates between Mach numbers and reduced frequencies. By this approach, "match-point" flutter speeds are obtained at selected altitudes.

### Flutter Analysis Results

In general, high margins of safety in flutter speed were predicted by the different models and methods. The correlation between the two methods as well as between free-free airplane and clamped component analysis was also good if the

same input data were used. Only for one set of preliminary mass data, considerable differences in flutter stability were found for the wing. Table 2 summarized results from this study.

The following sensitivities were investigated during the design phase:

- control surface attachment stiffness
- control surface mass moment of inertia
- control surface aerodynamic hinge moment coefficient
- fuselage flexibility due to buckled skins.

After the GVT, flutter analyses were performed with measured modes and frequencies after applying a smoothing process and updating the mass matrix.

#### Free - Play Flutter Analysis

Since the canard free-play requirement could not be met with one of the two actuators disconnected, a flutter analysis based on measured free-play was performed. For this condition, the effective attachment stiffness was calculated as a function of pitch amplitude, basic stiffness and free-play angle. Flutter analyses were then performed for a variation of the attachment stiffness down to the minimum flutter dynamic pressure requirement. For this condition, the maximum rotational amplitude was calculated. For this amplitude, the maximum canard displacement were obtained by the generalized flutter vector, transformed into the vibration degrees of freedom. For these displacements, the canard and support structure stresses and fatigue life were calculated. The results showed more than adequate flutter, strength, and fatigue margins of safety.

#### Buffet Response Design

Because the X-31A was designed for high angle of attack manoeuvres where vortical and separated flow conditions can excite the structure, especially the wing and vertical tail were examined carefully.

#### Wing Buffet

Although the wing response to buffet is alleviated by the wing leading edge flap deflection schedule - they are always deflected by the negative angle of attack up to a maximum of 40 degrees - an other potential buffet problem was discovered during the ground vibration test. Fig. 7 shows the first symmetric wing bending mode at 14.8 Hz, where the engine responds in pitch, and the engine pitch mode at 18.0 Hz where the wing responds in bending.

For this reason, a buffet response analysis was performed to determine especially the dynamic loads at the upper engine mount.

Valuable data for this analysis came from unsteady buffet measurements on a rigid wind tunnel model for a wing with a similar planform performed at DASA in 1981.

Based on this analysis, the initial engine mount design with thin aluminium plates was replaced by thicker gage steel parts.

#### Fin Buffet

Although wind tunnel streamline oil flow studies did not indicate the existence of forebody vortices or separated flow fields in the centerplane of the vertical tail that might induce fin buffet, the vertical tail to fuselage attachment

strength capability was increased above static strength requirements. This improvement resulted in a fail-safe design for the event that flight tests might reveal significant buffet excitations. In fact, initial flight with wing leading edge flaps not yet operating at the above described schedule, showed high acceleration levels at the fin tip.

### Ground Tests

#### Control Surface Free-Play Tests

To demonstrate that the required free-play limits from MIL-8870 are not exceeded, all control surfaces were tested under two different conditions: with both hydraulic systems operating and with only one hydraulic system active. These tests were performed by applying external loads in incremental step and in both directions to the control surfaces. The specified limits were met for all surfaces except for one condition: the tight requirement of 0.034 degrees for all-moving surfaces could not be met for the canard with one hydraulic system off. For this condition, the previously mentioned free-play flutter analysis was performed.

#### Ground Vibration Test

To verify and update the analytical dynamic model, a multiple shaker ground vibration test (GVT) was performed in late 1989. Table 3 summarizes the eigenmode frequencies for pre-GVT analysis, test results, and adjusted analysis values after the GVT.

The test was performed on soft tires instead of platform-type soft suspension system after analysis had indicated undesirable low-frequency platform modes due to the mass of the platforms.

### Structural Coupling Tests

To demonstrate the required stability margins for the digital flight control system (FCS) in the presence of the flexible structure, a structural coupling test (SCT), sometimes also called FCS-GVT, was performed for different conditions:

- open flight control loops
- closed control loops
- during taxi.

During these tests, the structure is not excited by external shakers. Frequency sweep inputs are generated by the flutter test box for the control surfaces. The response signals are then measured at the flight test accelerometers, at the inertia measurement unit, and at the feed-back signals to the control surfaces.

### Flutter Flight Test

#### Excitation System

To demonstrate flutter stability in flight, adequate excitation of all important structural modes is required. For the X-31A, the digital fly-by-wire flight control system provided an efficient opportunity low costs without changing the aircraft flutter characteristics. The only added hardware is the control box to command the desired oscillations or pulses through the flight control computer to the primary control surfaces. The possible control surface modes are:

- symmetric canard,
- rudder,
- wing trailing edge outboard flaps, symmetric and antisymmetric.

At all flight envelope test points, frequency sweeps between 0.1 and 100 Hz were generated. In addition, the pulse mode was also used for the canards to excite high frequency modes.

### Test Points

The test points plotted in fig. 8 were established to clear the flight envelope by incremental dynamic pressure lines with increasing Mach number and altitude steps. In the meantime, supersonic test points up to Mach 1.3 at high altitudes have been added and flutter stability could be demonstrated.

### Data Acquisition and Survey

The accelerometers depicted in fig. 9 were used to record the response signals during the tests. These signals were transmitted by telemetry to the ground station for on-line survey on multi-channel oscillographs and oscilloscopes. After checking these signals, the next point of flight test program could be cleared. Usually, between three and five test points on one dynamic pressure line could be test tested during each dedicated flutter flight.

### Test Data Analysis

The on-board tape accelerometer data were used after each flight for the evaluation of frequency and damping of the structural modes. A typical example of these results is presented in fig. 10.

Three different methods were used to determine the results. An average value for the damping from these three methods was then used to determine the safety to proceed to the next higher q-line.

All results showed more than adequate flutter stability margins, within the flight envelop as well as for the extrapolation to the chosen margin in speed.

### Conclusions

All objectives of the X-31A program could be met with great success. For this reason, an extension of the program is planned to test additional demanding fea-

tures like lateral stability without a vertical tail surface. The chosen approach with respect to aeroelasticity, for pre-design, design, ground-tests and the flight test program was also very successful. Sufficient aeroelastic stability as well as aeroelastic effectiveness were provided by a minimum effort in time and costs during all project phases.

In spite of the tight time schedule and the basic differences in analysis models and methods between the two partner companies, this program showed that a high-risk demonstrator project can successfully be completed - in spite of budgetary constraints - if appropriate assumptions are made at the beginning, if the data exchange between the partner companies is carefully planned, and if the flight test evaluation can be performed by efficient data acquisition, survey, and data analysis methods.

### References

- [1] Miller, J.: The X-Planes X-1 to X-31 Aerofax. Inc.; Arlington, Texas, 1988.
- [2] Robinson, M.R.; Herbst, Dr. W.B.: The X-31A and Advances Highly Manoeuvrable Aircraft. ICAS-Conference Proceedings: Stockholm, Sweden, 1990
- [3] Dobbs, S.K.; Hodson, C.H.; Shroyer, E.F.: Enhanced Fighter Manoeuvrability (X-31) Dynamic Design. ASME Annual Winter Conference; Dallas, Tx., 1990.
- [4] Gödel, H.: Recent Developments in Structural Optimisation with Respect to Dynamic and Aeroelastic Problems. C.P. International Forum on Aeroelasticity and Structural Dynamic. Aachen, Germany, 1991.

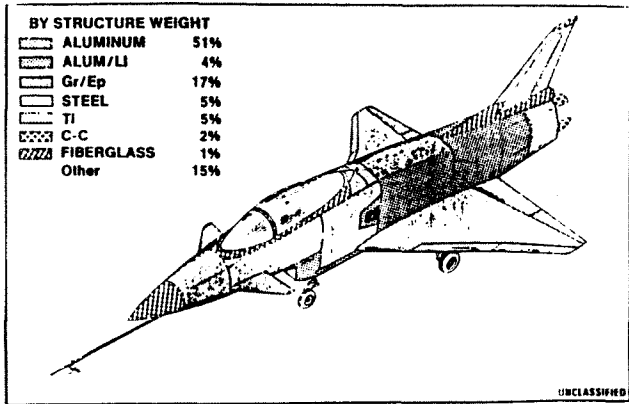


Fig.1 : X-31 A demonstrator aircraft

- : Doublet Lattice Analysis
- : CFD Analysis Results
- : Typical Flutter Wind Tunnel Model Trend

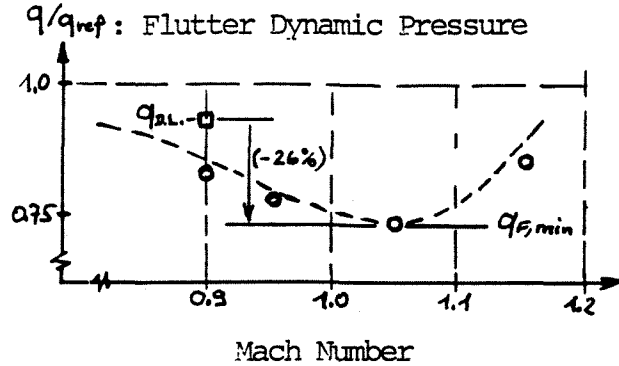


Fig.5 : Transonic Mach number effects on flutter speed

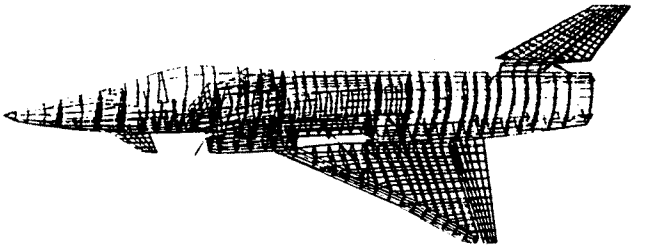


Fig.2 : Finite Element Model

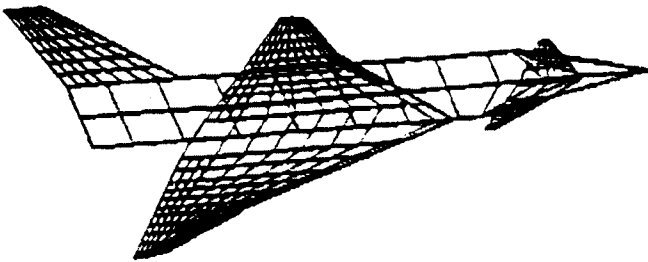


Fig.3 : Steady and unsteady aerodynamic model

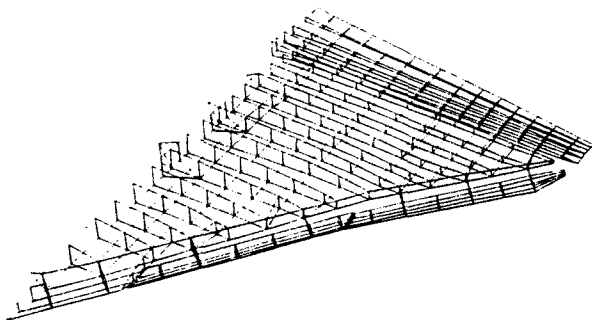


Fig.4 : Wing analysis model

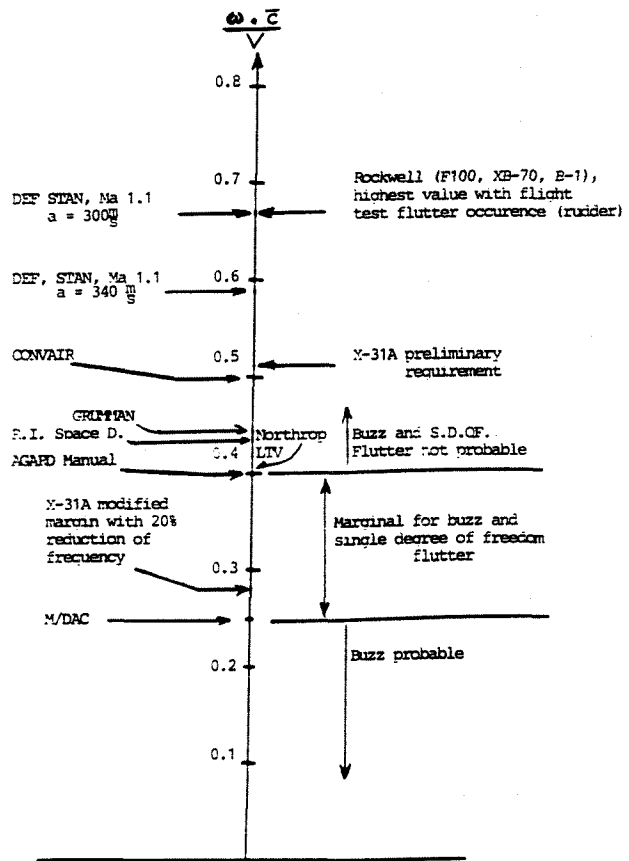


Fig.6 : Control surface buzz prevention criteria



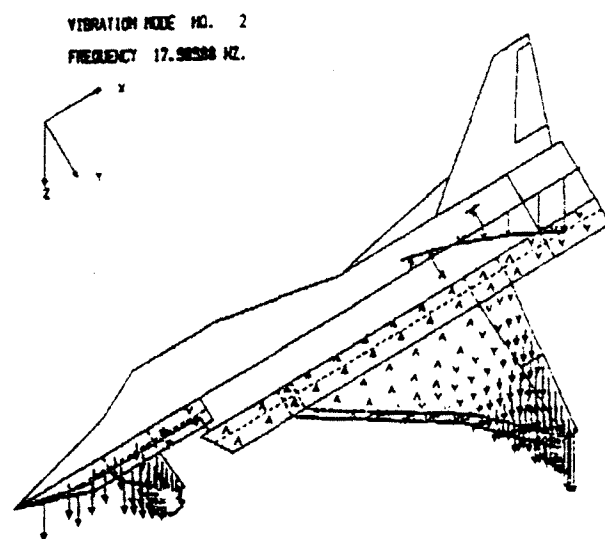
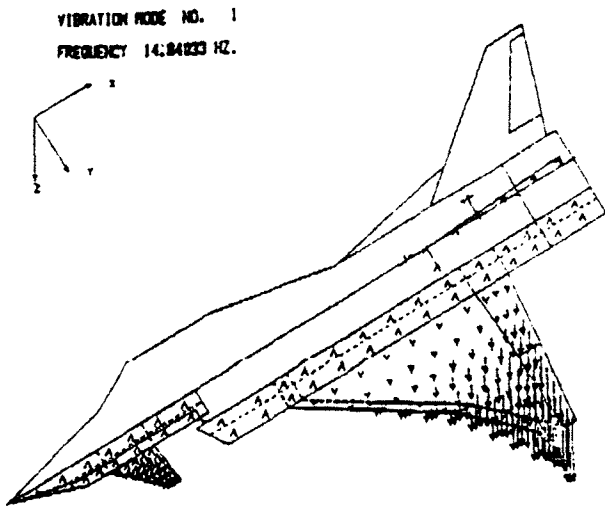


Fig 7: Symmetric wing and engine modes

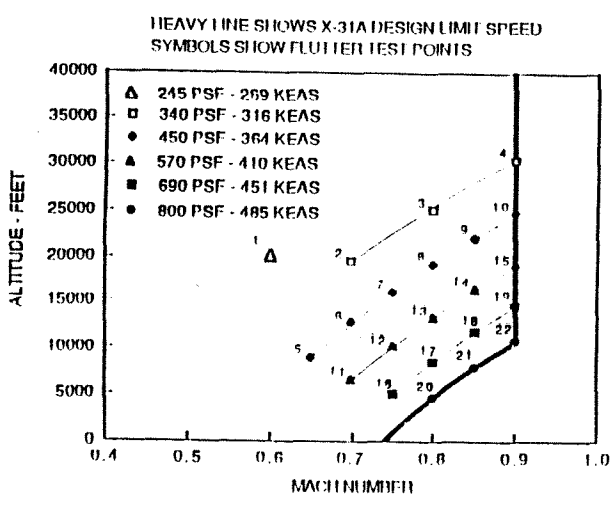


Fig 8: Flutter flight test points

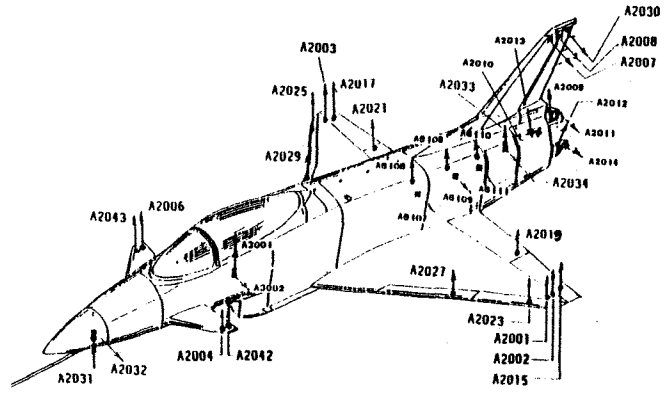


Fig 9: Flight test accelerometer location

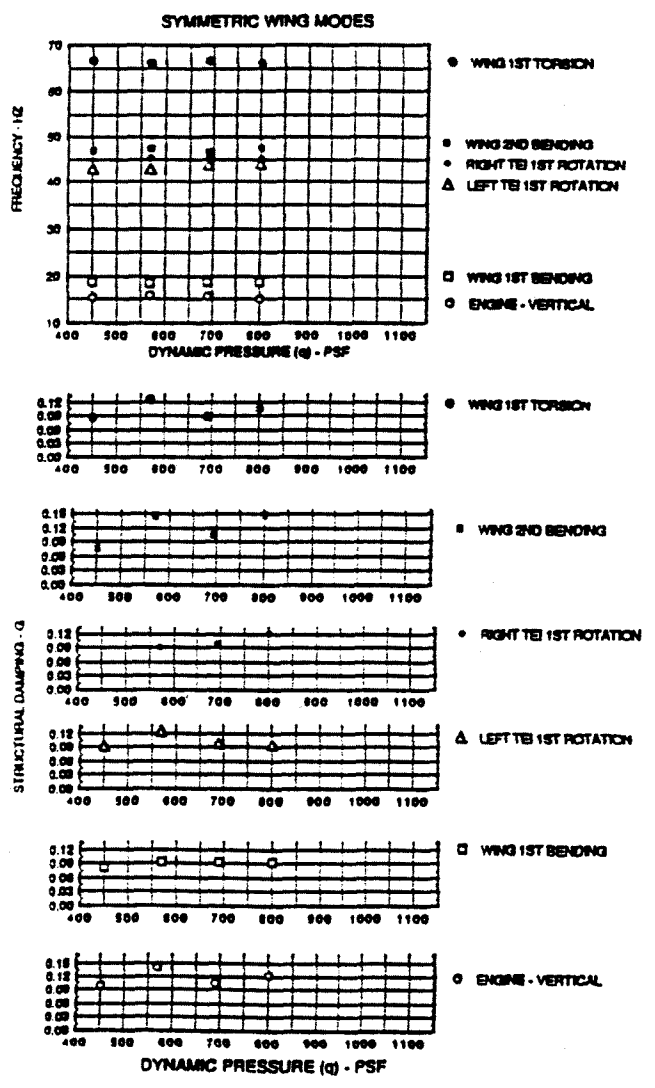


Fig 10a: Example of flight test results

Ma 0.9    q = 800 psf

$$\text{effectiveness} = \frac{\text{elastic value}}{\text{rigid value}}$$

$\alpha = 1 \text{ deg.}$	lift	flap lift	pitch moment	roll moment	hinge moment
total wing	0.95	-	0.94	0.94	-
L/E - I/B	1.31	1.01	-	-	1.01
L/E - O/B	1.64	1.04	-	-	1.04
L/E full span	1.55	1.04	-	-	-
T/E - I/B	0.80	0.93	-	0.76	0.92
T/E - O/B	0.69	0.88	-	0.71	0.79
T/E full span	0.75	0.89	-	0.73	0.86

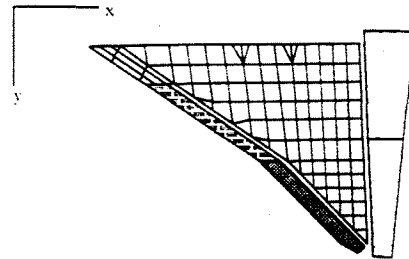


Table 1 : Static aeroelastic effectiveness results for the clamped wing

WING FLUTTER ANALYSIS RESULTS

Case	Flutter Frequency (Hz)	Flutter Mode No.	% Margin in Flutter q
<b>MBB NASTRAN FEM</b> Weight Distribution No. 2	60	4	209
<b>ROCKWELL ANALYSIS</b> Weight Distribution No. 1	54	4	38
Weight Distribution No. 2	60	4	217
Weight Distribution No. 1 with 15 lbs. on Tip	57	4	140
<b>WING ON COMPLETE AIRCRAFT</b> <b>Symmetric</b> Weight Distribution No. 1	30	12	13
Weight Distribution No. 2	24	3	405
<b>Antisymmetric</b> Weight Distribution No. 1	57	16	51
Weight Distribution No. 2	23	8	447

Weight Distribution No. 1 - Preliminary Wing Weight Distribution  
Weight Distribution No. 2 - Intermediate Wing Weight Distribution

Table 2 : Comparison of pre-and post GVT frequencies

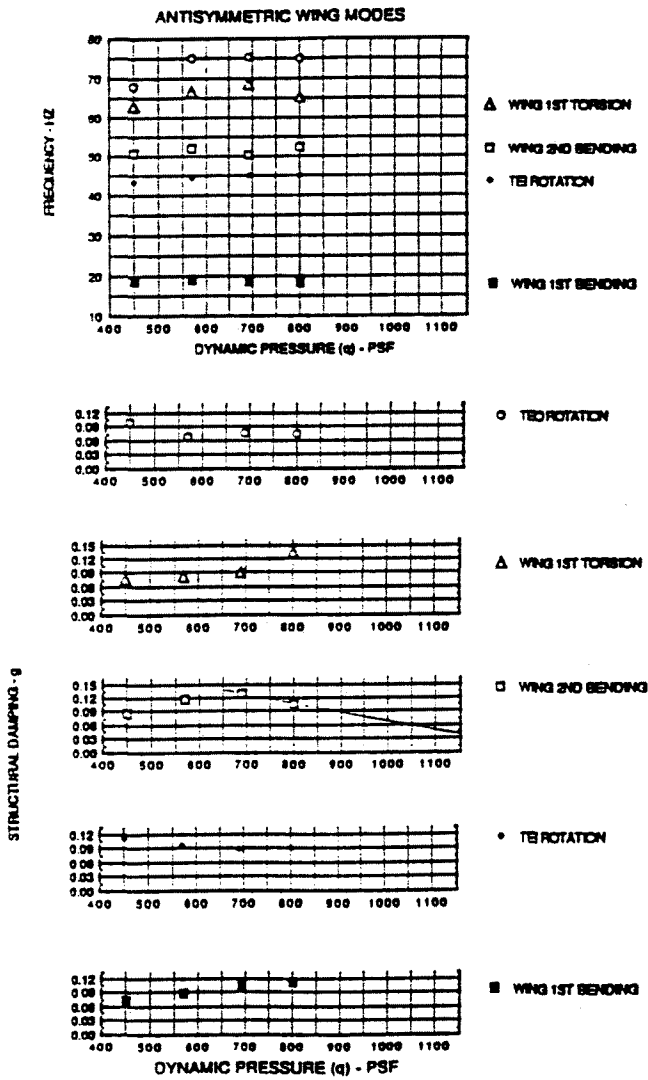


Fig 10b : Example of flight test results

MODE - ID	G V T	PREDIC- TED	ADJUS- TED
<u>Antisymmetric:</u>			
yaw	1.26	1.49	1.28
lateral	2.08	1.07	1.76
roll	6.02	4.19	6.23
engine	10.9	-	10.86
boom	13.7	5.38	13.61
wing 1 <sup>st</sup> bending	17.16	19.98	17.14
fuselage 1 <sup>st</sup> bending	22.3	18.20	21.43
vertical t. 1 <sup>st</sup> bending	25.5	25.10	23.61
fuselage 2 <sup>nd</sup> bending	31.23	37.68	32.81
wing 2 <sup>nd</sup> bending	47.68	43.91	39.36
fuselage torsion	44.0	35.17	43.63
trailing edge inboard	41.1	36.0	38.24
2 <sup>nd</sup> boom	-	-	49.67
canard 1 <sup>st</sup> bending	64.0	51.39	63.49
1 <sup>st</sup> rudder	60.0	53.18	54.25
wing 1 <sup>st</sup> torsion	63.7	55.09	59.07
trailing edge outboard	67.0	59.55	70.48
2 <sup>nd</sup> rudder	106.9	106.12	72.70
vertical t. 2 <sup>nd</sup> bending	83.2	68.88	110.37
canard torsion	127.7	124.47	132.37
leading edge outboard	128.8	74.64	127.64
leading edge inboard	144.9	78.46	138.00
canard 2 <sup>nd</sup> bending	150.0	133.41	152.00
vertical t. torsion	134.2	162.06	153.98

MODE - ID	G V T	PREDIC- TED	ADJUS- TED
<u>Symmetric:</u>			
Pitch	1.87	1.31	1.86
Plunge	4.00	2.70	3.91
Boom	12.89	5.58	12.93
Wing 1 <sup>st</sup> bending	14.17	17.02	14.87
Engine pitch	17.93	-	18.01
Fuselage 1 <sup>st</sup> bending	24.70	14.68	23.84
Trailing edge inboard	38.90	35.99	37.89
Fuselage 2 <sup>nd</sup> bending	-	28.76	40.13
wing 2 <sup>nd</sup> bending	45.80	42.08	42.19
2 <sup>nd</sup> boom	55.80	40.01	52.89
fuselage/engine	-	53.72	-
wing torsion	61.30	57.53	57.56
canard 1 <sup>st</sup> bending	60.10	45.67	51.42
trailing edge outboard	66.90	61.64	70.99
fuselage 3 <sup>rd</sup> bending	69.20	46.75	77.49
wing 3 <sup>rd</sup> bending	99.50	73.00	104.85
canard torsion	110.40	77.73	107.30
leading edge outboard	125.80	82.14	125.70
leading edge inboard	139.50	79.00	136.20
canard 2 <sup>nd</sup> bending	144.80	140.38	148.70

**Table 3 : Comparison of pre- and post GVT frequencies (symmetric)**

**Table 3 : Comparison of pre- and post GVT frequencies (antisymmetric)**